



香港中文大學

The Chinese University of Hong Kong

# VLSI Mask Optimization: From Shallow To Deep Learning

Bei Yu

Department of Computer Science & Engineering

Chinese University of Hong Kong

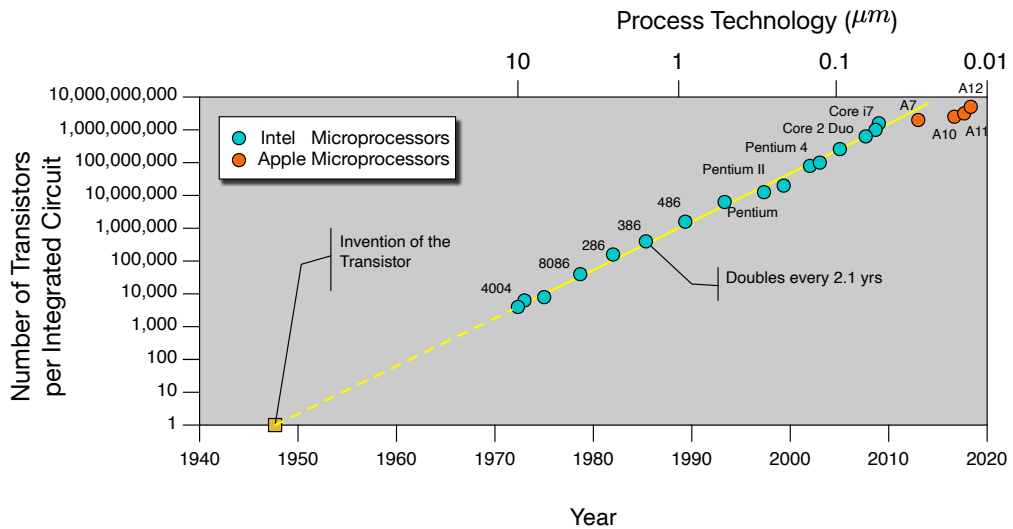
[byu@cse.cuhk.edu.hk](mailto:byu@cse.cuhk.edu.hk)

August 9, 2021

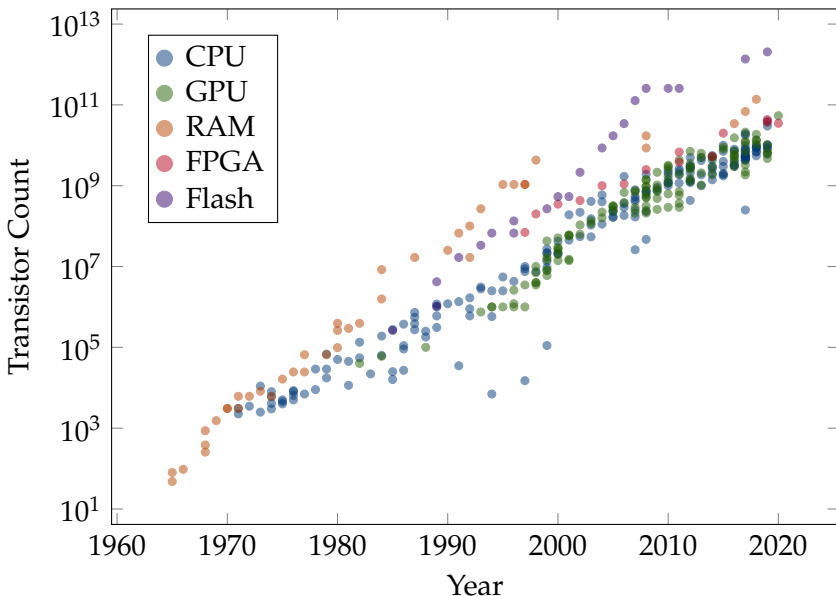
# Moore's Law to Extreme Scaling



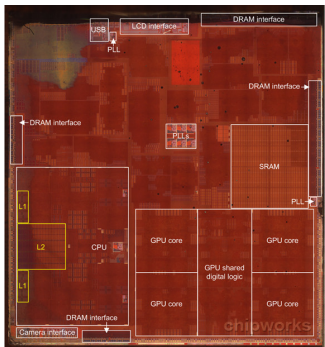
## Moore's Law



# Moore's Law to Extreme Scaling

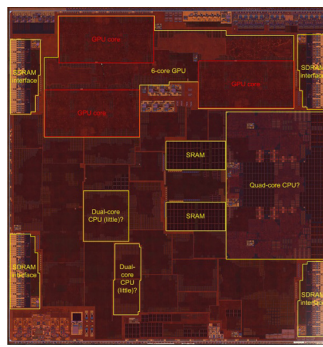


# Scaling of Apple SOC



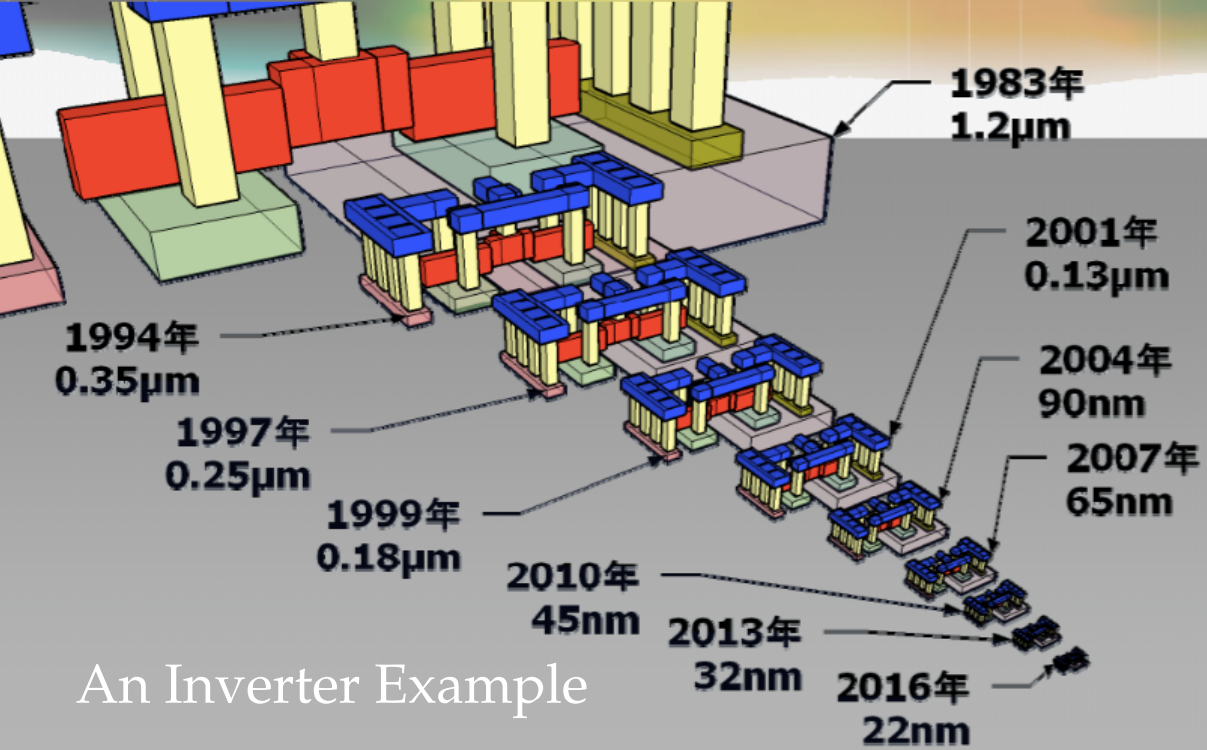
Apple A7 (2013)

- 1,000,000,000 Transistors
- $102\text{mm}^2$  die size
- 1.3GHz



Apple A10 (2016)

- 3,300,000,000 Transistors
- $125\text{mm}^2$  die size
- 2.34GHz



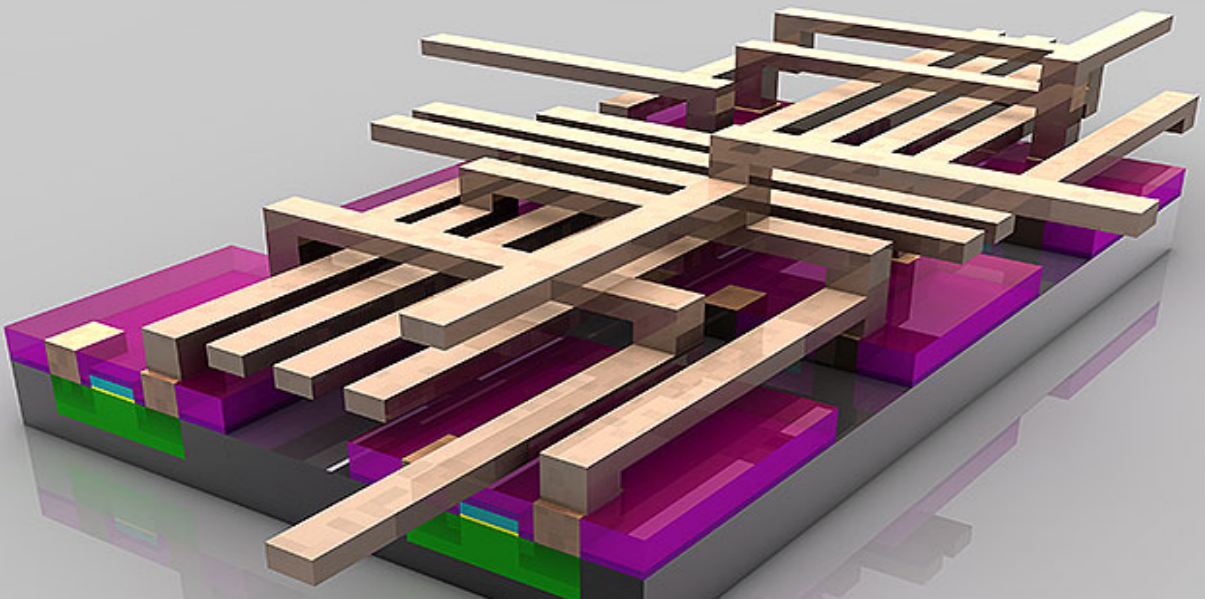
# 2005



# 2014

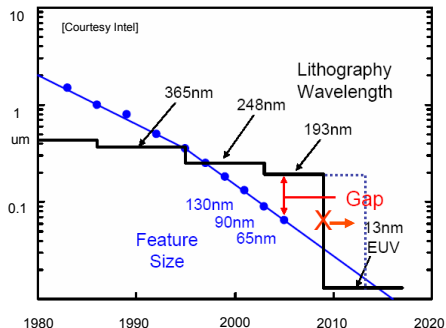
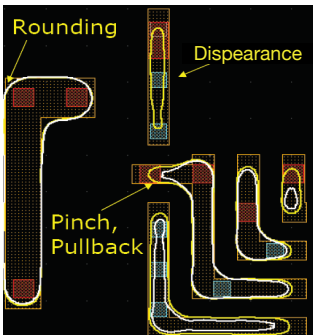


Memory Card Scaling



Detailed View of Layout

# Manufacturing Issues of Layout



Manufacturability Status & Challenges



Market Anually: USD 100M!

- ① Calibre by Mentor Graphics
- ② Brion Tool by ASML
- ③ IC Validator by Synopsys
- ④ Pegasus by Cadence

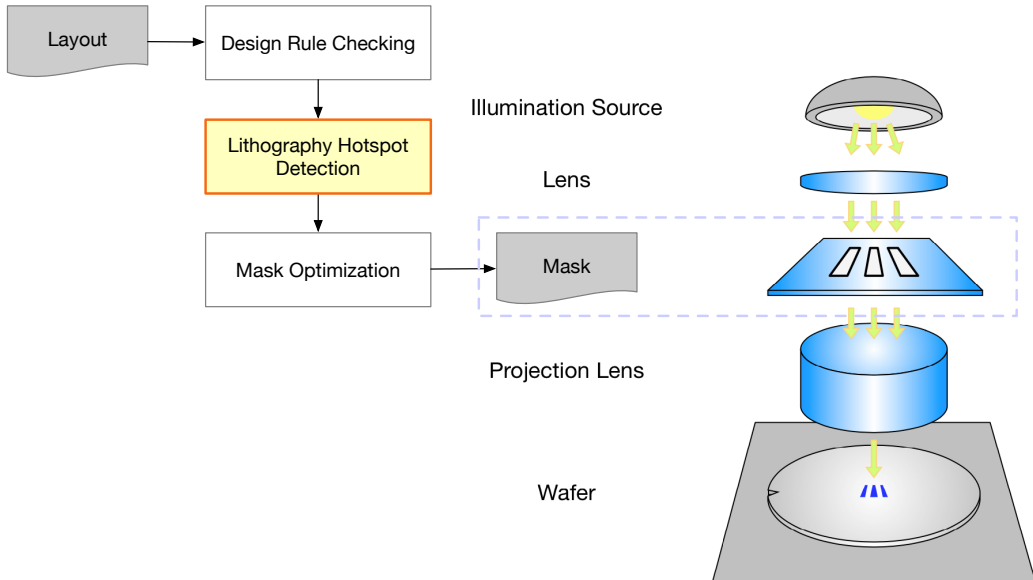
**Mentor**<sup>®</sup>

A Siemens Business

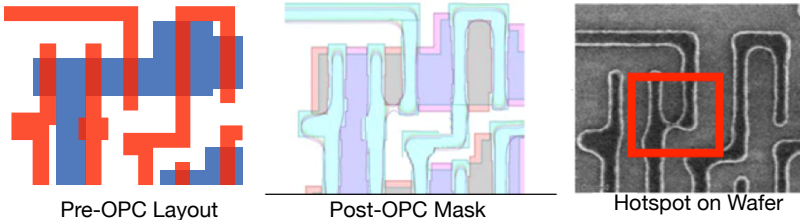
**BRION**  
an **ASML** company

**SYNOPSYS**<sup>®</sup> **cadence**

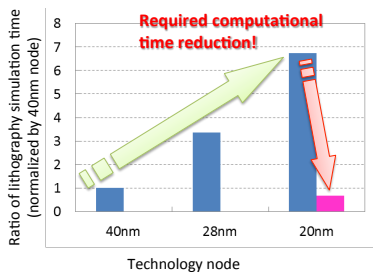
# Hotspot Detection



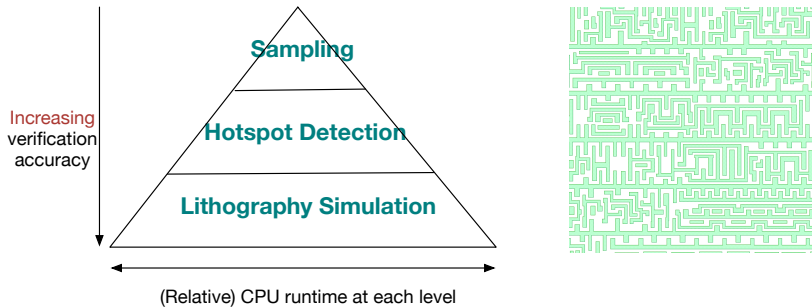
# Challenge: Failure (Hotspot) Detection



- RET: OPC, SRAF, MPL
- Still hotspot: low fidelity patterns
- Simulations: **extremely** CPU intensive

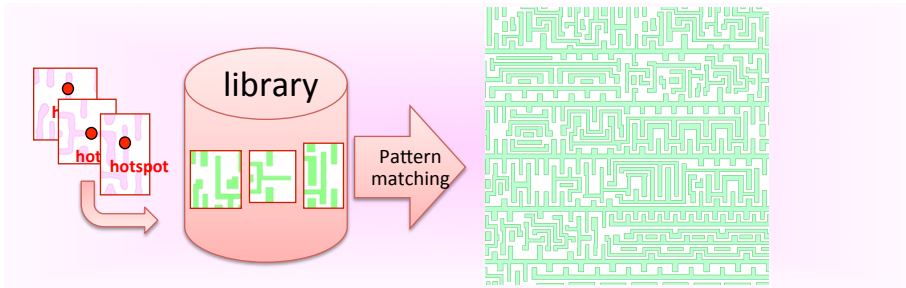


# Hotspot Detection Hierarchy

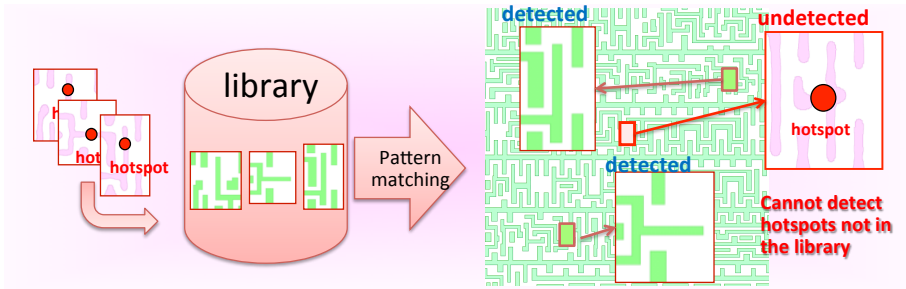


- **Sampling** (DRC Checking):  
scan and rule check each region
- **Hotspot Detection:**  
verify the sampled regions and report potential hotspots
- **Lithography Simulation:**  
final verification on the reported hotspots

# Pattern Matching based Hotspot Detection

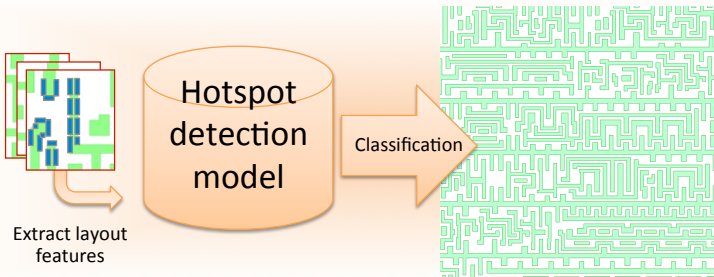


# Pattern Matching based Hotspot Detection

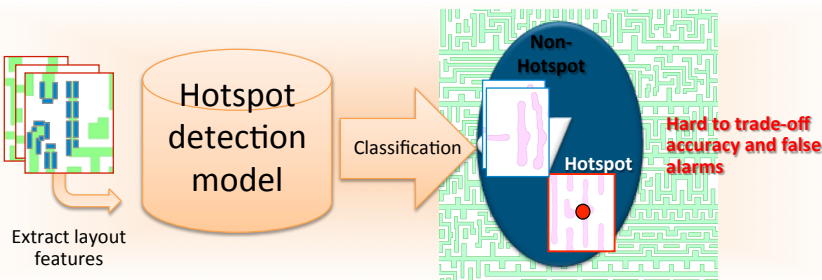


- Fast and accurate
- [Yu+, ICCAD'14] [Nosato+, JM3'14] [Su+, TCAD'15]
- Fuzzy pattern matching [Wen+, TCAD'14]
- Hard to detect non-seen pattern

# Classification based Hotspot Detection



# Classification based Hotspot Detection

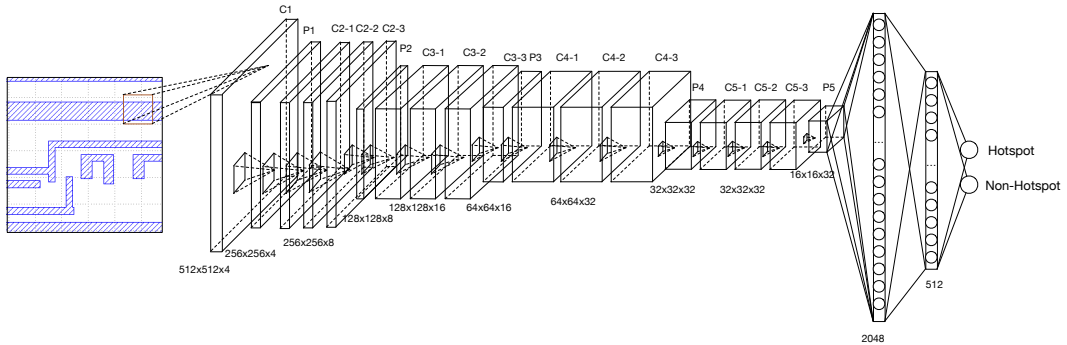


- Predict new patterns
- Decision-tree, ANN, SVM, Boosting ...
- [Drmanac+, DAC'09] [Ding+, TCAD'12] [Yu+, JM3'15] [Matsunawa+, SPIE'15] [Yu+, TCAD'15]
- **Hard** to balance accuracy and false-alarm

# First DNN Hotspot Detection Architecture<sup>1</sup>



- Total 21 layers with 13 convolution layers and 5 pooling layers.
- A ReLU is applied after each convolution layer.

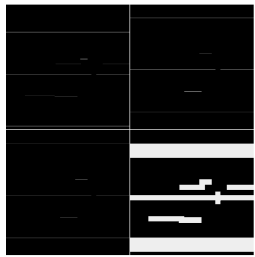


<sup>1</sup>Haoyu Yang, Luyang Luo, et al. (2017). "Imbalance aware lithography hotspot detection: a deep learning approach". In: JM3 16.3, p. 033504.

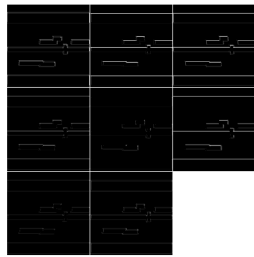
# Layer Visualization



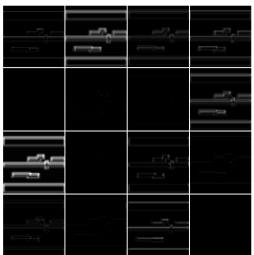
Origin



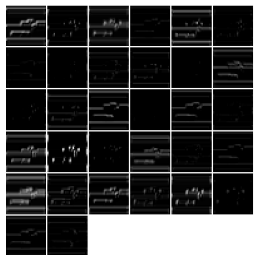
Pool1



Pool2



Pool3

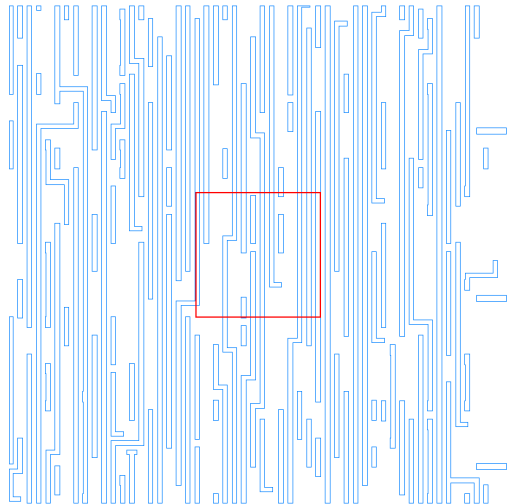


Pool4

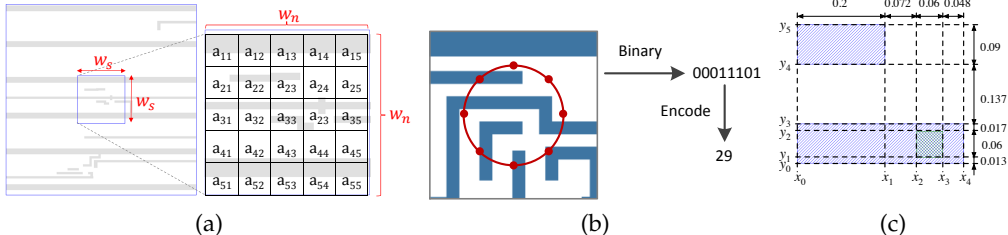


Pool5

# Rethinking: “ImageHotspot” v.s. ImageNet



# HSD-Research: New Representation



- (a) Density-based encoding [SPIE'15]<sup>2</sup>
- (b) Concentric circle sampling [ICCAD'16]<sup>3</sup>
- (c) Squish pattern [ASPDAC'19]<sup>4</sup>

<sup>2</sup>Tetsuaki Matsunawa et al. (2015). "A new lithography hotspot detection framework based on AdaBoost classifier and simplified feature extraction". In: *Proc. SPIE*. vol. 9427.

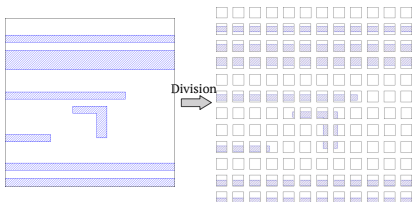
<sup>3</sup>Hang Zhang, Bei Yu, and Evangeline F. Y. Young (2016). "Enabling Online Learning in Lithography Hotspot Detection with Information-Theoretic Feature Optimization". In: *Proc. ICCAD*, 47:1–47:8.

<sup>4</sup>Haoyu Yang, Piyush Pathak, et al. (2019). "Detecting multi-layer layout hotspots with adaptive squish patterns". In: *Proc. ASPDAC*, pp. 299–304.



## Feature Tensor Generation:

- Clip Partition
- Discrete Cosine Transform
- Discarding High Frequency Components
- Feature Tensor

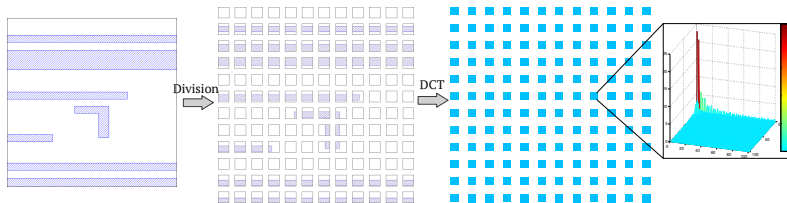


<sup>5</sup>Haoyu Yang, Jing Su, et al. (2017). "Layout Hotspot Detection with Feature Tensor Generation and Deep Biased Learning". In: *Proc. DAC*, 62:1–62:6.



## Feature Tensor Generation:

- Clip Partition
- Discrete Cosine Transform
- Discarding High Frequency Components
- Feature Tensor

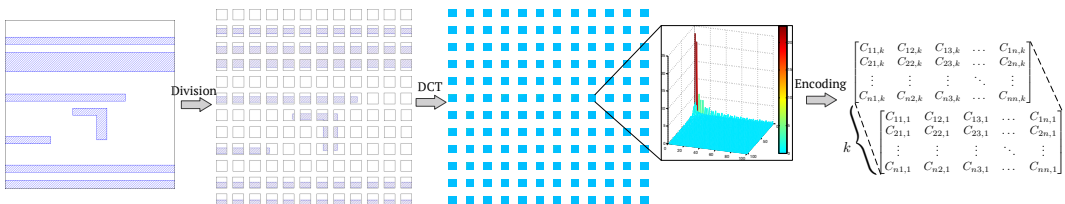


<sup>5</sup>Haoyu Yang, Jing Su, et al. (2017). "Layout Hotspot Detection with Feature Tensor Generation and Deep Biased Learning". In: *Proc. DAC*, 62:1–62:6.



## Feature Tensor Generation:

- Clip Partition
- Discrete Cosine Transform
- Discarding High Frequency Components
- Feature Tensor



<sup>5</sup>Haoyu Yang, Jing Su, et al. (2017). "Layout Hotspot Detection with Feature Tensor Generation and Deep Biased Learning". In: *Proc. DAC*, 62:1–62:6.

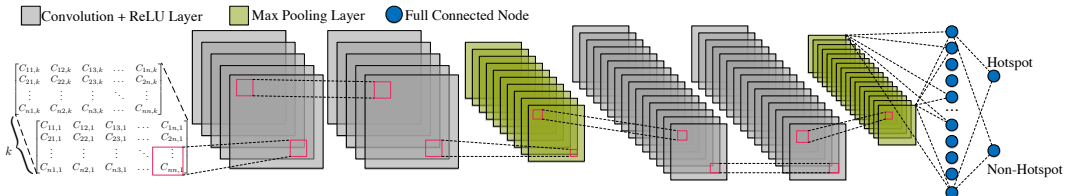
# Simplified CNN Architecture [DAC'17]



## Feature Tensor

- $k$ -channel hyper-image
- Compatible with CNN
- Storage and computational efficiency

Layer	Kernel Size	Stride	Output Node #
conv1-1	3	1	$12 \times 12 \times 16$
conv1-2	3	1	$12 \times 12 \times 16$
maxpooling1	2	2	$6 \times 6 \times 16$
conv2-1	3	1	$6 \times 6 \times 32$
conv2-2	3	1	$6 \times 6 \times 32$
maxpooling2	2	2	$3 \times 3 \times 32$
fc1	N/A	N/A	250
fc2	N/A	N/A	2



# The Biased Learning Algorithm



- Minimize difference with ground truths

$$\mathbf{y}_n^* = [1, 0], \mathbf{y}_h^* = [0, 1].$$

$$F \in \begin{cases} \mathcal{N}, & \text{if } \mathbf{y}(0) > 0.5, \\ \mathcal{H}, & \text{if } \mathbf{y}(1) > 0.5. \end{cases}$$

- Naive: Shifting decision boundary

$$F \in \begin{cases} \mathcal{N}, & \text{if } \mathbf{y}(0) > 0.5 + \lambda, \\ \mathcal{H}, & \text{if } \mathbf{y}(1) > 0.5 - \lambda. \end{cases}$$

# The Biased Learning Algorithm



- Minimize difference with ground truths

$$\mathbf{y}_n^* = [1, 0], \mathbf{y}_h^* = [0, 1].$$

$$F \in \begin{cases} \mathcal{N}, & \text{if } \mathbf{y}(0) > 0.5, \\ \mathcal{H}, & \text{if } \mathbf{y}(1) > 0.5. \end{cases}$$

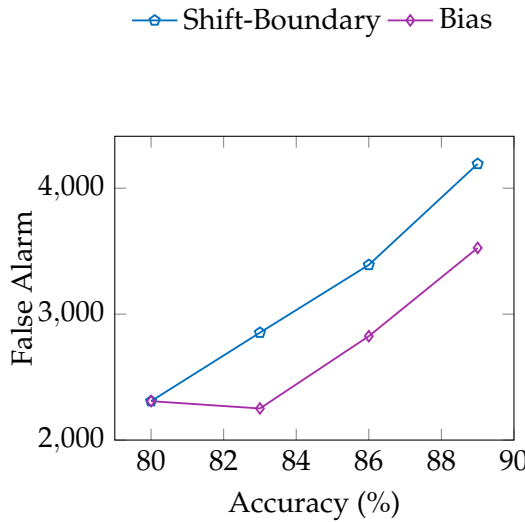
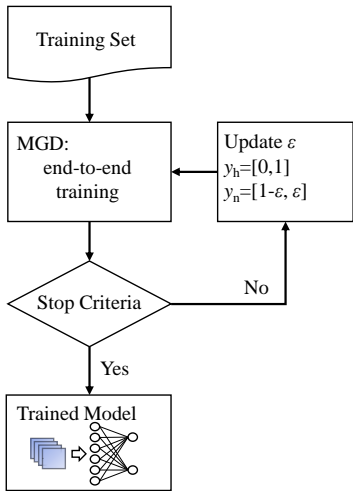
- Naive: Shifting decision boundary ( $\times$ )

$$F \in \begin{cases} \mathcal{N}, & \text{if } \mathbf{y}(0) > 0.5 + \lambda, \\ \mathcal{H}, & \text{if } \mathbf{y}(1) > 0.5 - \lambda. \end{cases}$$

- Biased ground truth:

$$\mathbf{y}_n^* = [1 - \epsilon, \epsilon].$$

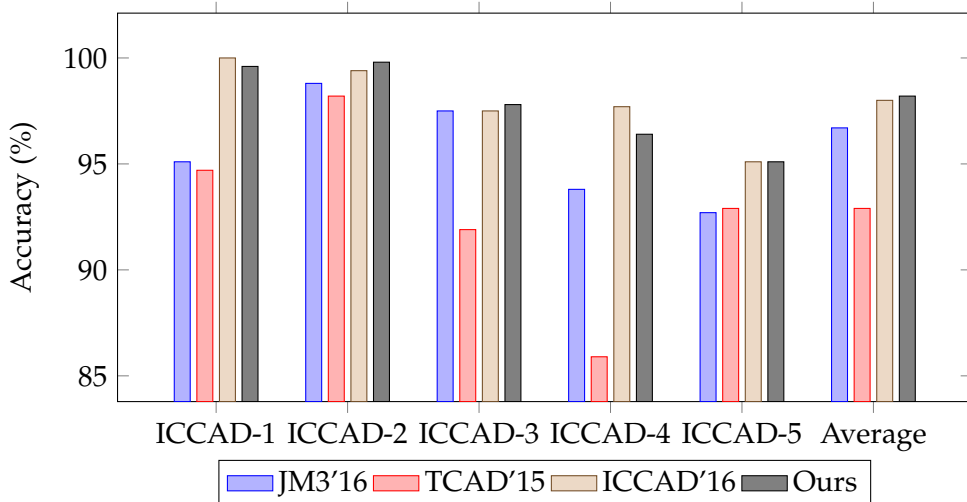
# The Biased Learning Algorithm



# Comparison with Previous Hotspot Detectors



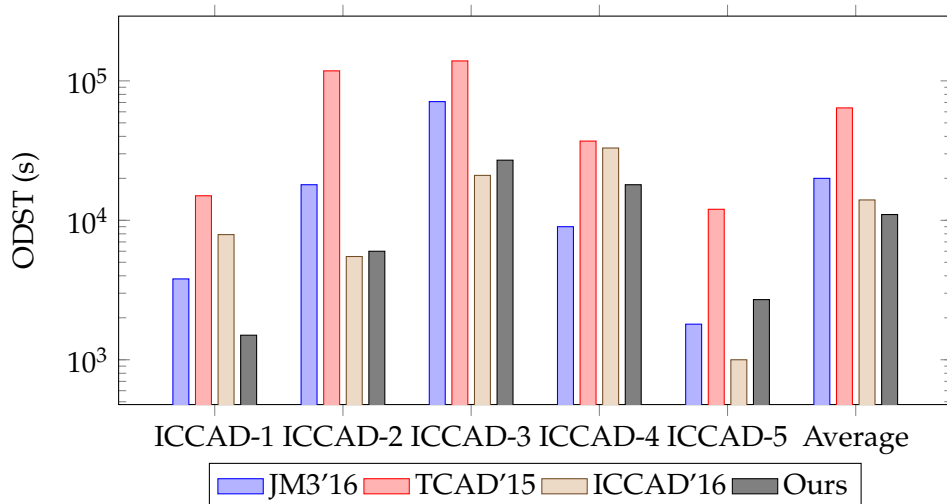
- Detection accuracy improved from 89.6% to 95.5%



# Comparison with Previous Hotspot Detectors



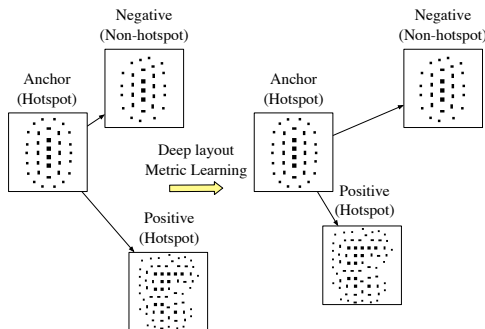
- Comparable false alarm penalty





## Motivation

- In original space, the anchor is much similar to the negative
- After deep layout metric learning, in a new manifold, the two hotspot layout clips are kept apart from the non-hotspot clip



<sup>6</sup>Hao Geng, Haoyu Yang, et al. (2020). "Hotspot Detection via Attention-based Deep Layout Metric Learning". In: *Proc. ICCAD*.

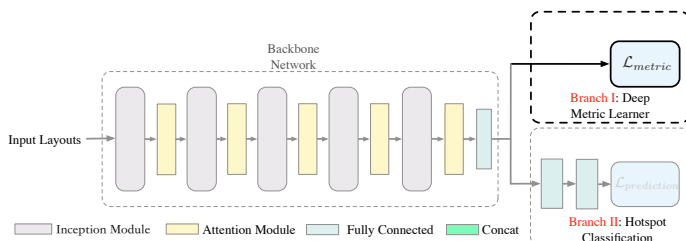
# Metric Feature Learning



- A triplet:  $f_w(\mathbf{x}_i), f_w(\mathbf{x}_i^+), f_w(\mathbf{x}_i^-)$
- $f_w(\mathbf{x}_i)$ : an anchor layout clip
- $f_w(\mathbf{x}_i^+)$ : sharing the same label with the anchor
- $f_w(\mathbf{x}_i^-)$ : having the opposite label to the anchor

$$\min_w \frac{1}{n} \sum_{i=1}^N \max(0, M + \|f_w(\mathbf{x}_i) - f_w(\mathbf{x}_i^+)\|_2^2 - \|f_w(\mathbf{x}_i) - f_w(\mathbf{x}_i^-)\|_2^2) \quad (1)$$

$$\text{s.t. } \|f_w(\mathbf{x}_i)\|_2^2 = 1, \forall (f_w(\mathbf{x}_i), f_w(\mathbf{x}_i^+), f_w(\mathbf{x}_i^-)) \in \mathcal{T}. \quad (2)$$



# Metric Feature Learning



Gradients Calculation:

$$\begin{aligned} \frac{\partial \mathcal{L}_{metric}(f_w(\mathbf{x}_i), f_w(\mathbf{x}_i^+), f_w(\mathbf{x}_i^-))}{\partial f_w(\mathbf{x}_i^+)} &= \frac{2}{n} (f_w(\mathbf{x}_i^+) - f_w(\mathbf{x}_i)) \\ &\cdot \mathbf{1} (\mathcal{L}_{metric}(f_w(\mathbf{x}_i), f_w(\mathbf{x}_i^+), f_w(\mathbf{x}_i^-)) > 0), \end{aligned} \quad (3a)$$

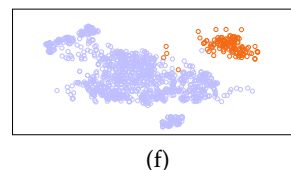
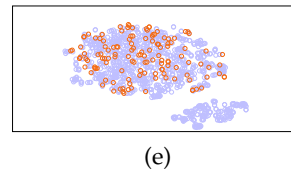
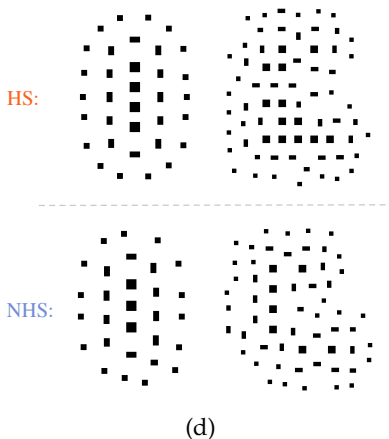
$$\begin{aligned} \frac{\partial \mathcal{L}_{metric}(f_w(\mathbf{x}_i), f_w(\mathbf{x}_i^+), f_w(\mathbf{x}_i^-))}{\partial f_w(\mathbf{x}_i^-)} &= \frac{2}{n} (f_w(\mathbf{x}_i) - f_w(\mathbf{x}_i^-)) \\ &\cdot \mathbf{1} (\mathcal{L}_{metric}(f_w(\mathbf{x}_i), f_w(\mathbf{x}_i^+), f_w(\mathbf{x}_i^-)) > 0), \end{aligned} \quad (3b)$$

$$\begin{aligned} \frac{\partial \mathcal{L}_{metric}(f_w(\mathbf{x}_i), f_w(\mathbf{x}_i^+), f_w(\mathbf{x}_i^-))}{\partial f_w(\mathbf{x}_i)} &= \frac{2}{n} (f_w(\mathbf{x}_i^-) - f_w(\mathbf{x}_i^+)) \\ &\cdot \mathbf{1} (\mathcal{L}_{metric}(f_w(\mathbf{x}_i), f_w(\mathbf{x}_i^+), f_w(\mathbf{x}_i^-)) > 0), \end{aligned} \quad (3c)$$

where  $\mathbf{1}$  is the indicator function which is defined as:

$$\mathbf{1}(x) = \begin{cases} 1 & \text{if } x \text{ is true,} \\ 0 & \text{otherwise.} \end{cases} \quad (3d)$$

# The t-SNE visualizations of feature embeddings on VIA benchmark

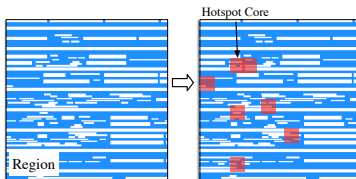


- (a) The exemplars of hotspots and non-hotspots; (b) The DCT feature embeddings of TCAD'19; (c) The feature embeddings of our proposed framework.

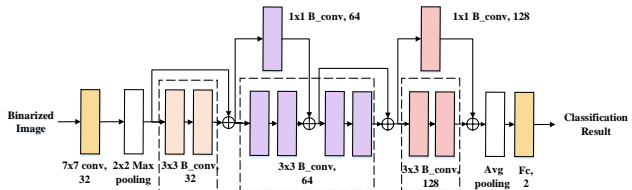
# HSD-Research: New Network Architecture



- Region-based HSD [DAC'19]<sup>7</sup>



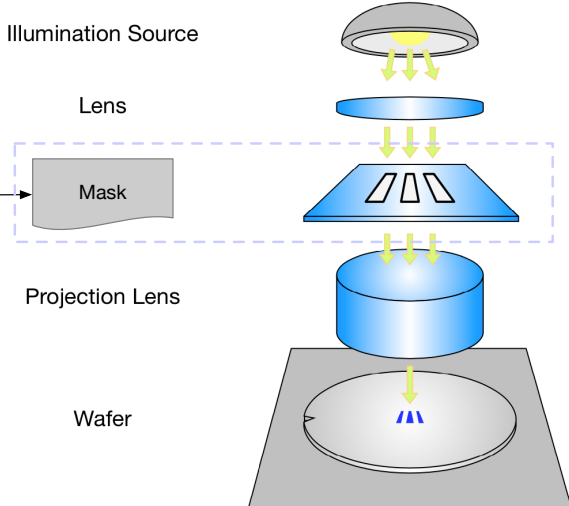
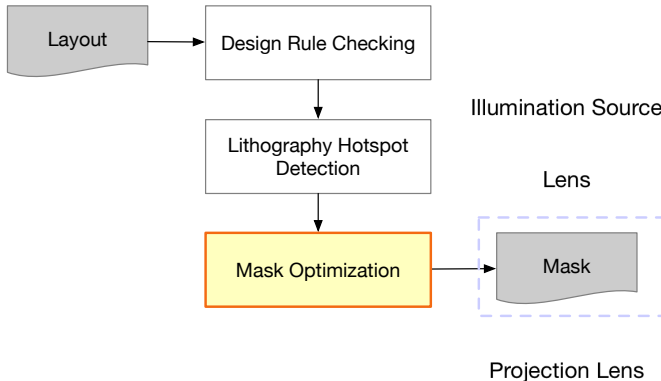
- Binarized residual neural network [DAC'19]<sup>8</sup>



<sup>7</sup>Ran Chen et al. (2019). "Faster Region-based Hotspot Detection". In: *Proc. DAC*, 146:1–146:6.

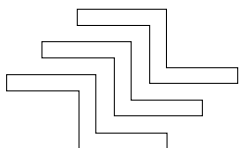
<sup>8</sup>Yiyang Jiang et al. (2019). "Efficient Layout Hotspot Detection via Binarized Residual Neural Network". In: *Proc. DAC*, 147:1–147:6.

# Mask Optimization





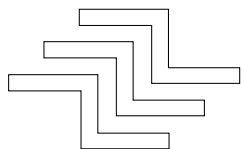
Design target



# Mask Optimization



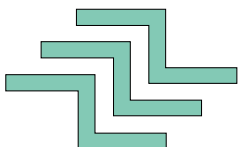
Design target



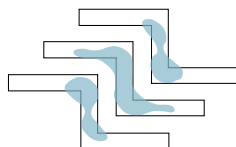
without OPC



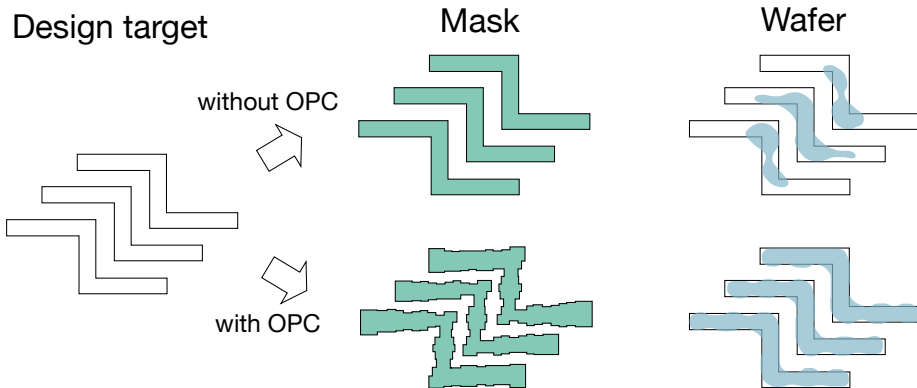
Mask



Wafer



# Mask Optimization





Market Anually: USD 100M!

- ① Calibre by Mentor Graphics
- ② Brion Tool by ASML
- ③ IC Validator by Synopsys
- ④ Pegasus by Cadence

**Mentor®**  
A Siemens Business

**BRION**  
an **ASML** company

**SYNOPSYS®** cādence

# Lithography Model



- SVD Approximation of Partial Coherent System [Cobb,1998]

$$\mathbf{I} = \sum_{k=1}^{N^2} w_k |\mathbf{M} \otimes \mathbf{h}_k|^2. \quad (4)$$

- Reduced Model [Gao+,DAC'14]

$$\mathbf{I} = \sum_{k=1}^{N_h} w_k |\mathbf{M} \otimes \mathbf{h}_k|^2. \quad (5)$$

- Etch Model

$$\mathbf{Z}(x, y) = \begin{cases} 1, & \text{if } \mathbf{I}(x, y) \geq I_{th}, \\ 0, & \text{if } \mathbf{I}(x, y) < I_{th}. \end{cases} \quad (6)$$

# Inverse Lithography Technique (ILT)



The main objective in ILT is minimizing the lithography error through gradient descent.

$$E = \|\mathbf{Z}_t - \mathbf{Z}\|_2^2, \quad (7)$$

where  $\mathbf{Z}_t$  is the target and  $\mathbf{Z}$  is the wafer image of a given mask.

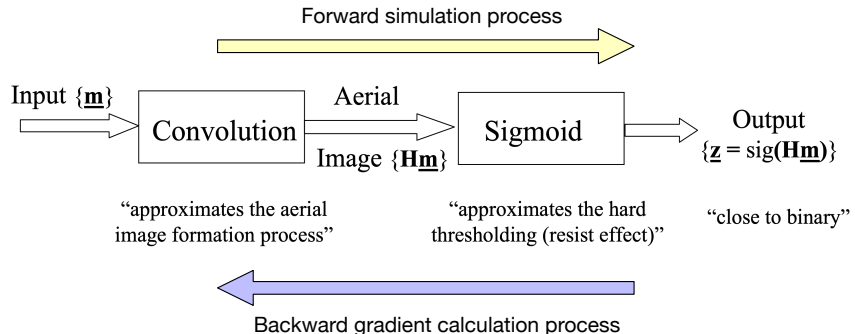
Apply translated sigmoid functions to make the pixel values close to either 0 or 1.

$$\mathbf{Z} = \frac{1}{1 + \exp[-\alpha \times (\mathbf{I} - \mathbf{I}_{th})]}, \quad (8)$$

$$\mathbf{M}_b = \frac{1}{1 + \exp(-\beta \times \mathbf{M})}. \quad (9)$$

Combine Equations (4)–(9) and the analysis in [Poonawala,TIP'07],

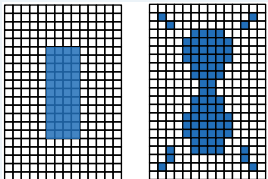
$$\begin{aligned} \frac{\partial E}{\partial \mathbf{M}} = & 2\alpha\beta \times \mathbf{M}_b \odot (1 - \mathbf{M}_b) \odot \\ & (((\mathbf{Z} - \mathbf{Z}_t) \odot \mathbf{Z} \odot (1 - \mathbf{Z}) \odot (\mathbf{M}_b \otimes \mathbf{H}^*)) \otimes \mathbf{H} + \\ & ((\mathbf{Z} - \mathbf{Z}_t) \odot \mathbf{Z} \odot (1 - \mathbf{Z}) \odot (\mathbf{M}_b \otimes \mathbf{H})) \otimes \mathbf{H}^*). \end{aligned} \quad (10)$$





## Typical ILT

- Mask → Image → Matrix
- Calculate gradient on each pixel.



## Level-set method

- Boundary-based update
- Implicit representation; focus on boundaries

$$\begin{cases} \phi(t, x) < 0 & \text{if } x \in \Omega(t) \\ \phi(t, x) = 0 & \text{if } x \in \Gamma(t) \\ \phi(t, x) > 0 & \text{if } x \in \overline{\Omega(t)} \end{cases}$$

<sup>1</sup>Jhih-Rong Gao et al. (2014). "MOSAIC: Mask Optimizing Solution With Process Window Aware Inverse Correction". In: *Proc. DAC*. San Jose, California, 52:1–52:6.

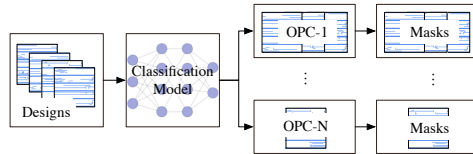
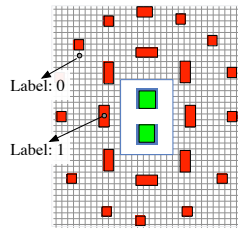
<sup>2</sup>Yuzhe Ma et al. (2017). "A Unified Framework for Simultaneous Layout Decomposition and Mask Optimization". In: *Proc. ICCAD*, pp. 81–88.

<sup>3</sup>Ziyang Yu et al. (2021). "A GPU-enabled Level Set Method for Mask Optimization". In: *Proc. DATE*.



## Discriminative models [TCAD'20]<sup>4</sup> [ASPDAC'20]<sup>5</sup>

- Pixel-wise classification
- Printed image estimation/quality estimation



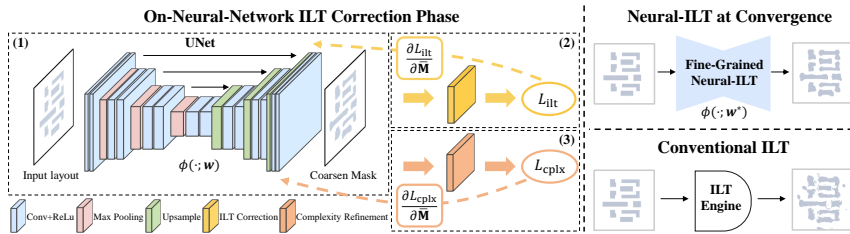
<sup>4</sup>Hao Geng, Wei Zhong, et al. (2020). "SRAF Insertion via Supervised Dictionary Learning". In: *IEEE TCAD*.

<sup>5</sup>Haoyu Yang, Wei Zhong, et al. (2020). "VLSI Mask Optimization: From Shallow To Deep Learning". In: *Proc. ASPDAC*, pp. 434–439.



## Generative model [DAC'18]<sup>6</sup> [ICCAD'20]<sup>7</sup> [ICCAD'20]<sup>8</sup>

- Image generation

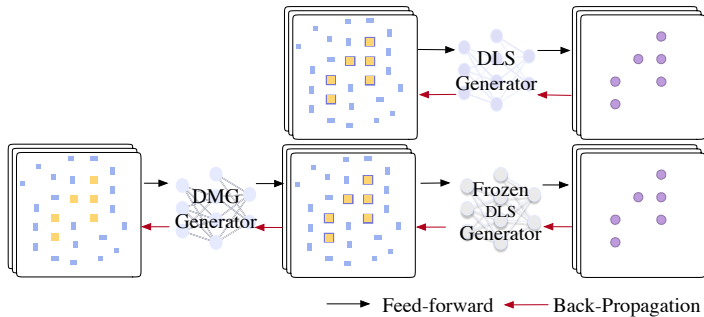


<sup>6</sup>Haoyu Yang, Shuhe Li, et al. (2018). “GAN-OPC: Mask Optimization with Lithography-guided Generative Adversarial Nets”. In: *Proc. DAC*, 131:1–131:6.

<sup>7</sup>Bentian Jiang et al. (2020). “Neural-ILT: Migrating ILT to Neural Networks for Mask Printability and Complexity Co-optimization”. In: *Proc. ICCAD*.

<sup>8</sup>Guojin Chen et al. (2020). “DAMO: Deep Agile Mask Optimization for Full Chip Scale”. In: *Proc. ICCAD*.

# Deep Mask Optimization [ICCAD'20]<sup>8</sup>



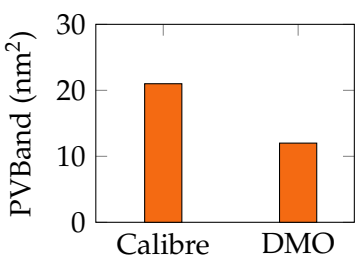
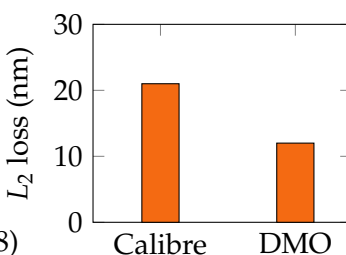
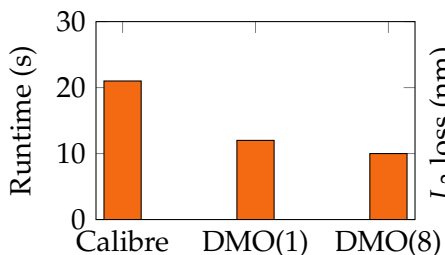
	GAN-OPC			Calibre			DMO		
	$L_2$ (nm)	PV Band (nm <sup>2</sup> )	Runtime (s)	$L_2$ (nm)	PV Band (nm <sup>2</sup> )	Runtime (s)	$L_2$ (nm)	PV Band (nm <sup>2</sup> )	Runtime (s)
case 1	7456	11424	284	5159	11671	1417	<b>4631</b>	<b>11166</b>	352
case 2	7321	11215	281	4987	11463	1406	<b>4432</b>	<b>10955</b>	336
case 3	7102	11265	285	5420	11516	1435	<b>4802</b>	<b>11032</b>	367
case 4	8032	11642	322	5382	11910	1606	<b>4835</b>	<b>11265</b>	399
Average	7478	11386	293	5237	11640	1466	<b>4675</b>	<b>11104</b>	363
Ratio	1.60	1.03	0.80	1.12	1.05	4.04	<b>1.00</b>	<b>1.00</b>	1.00

<sup>8</sup>Guojin Chen et al. (2020). "DAMO: Deep Agile Mask Optimization for Full Chip Scale". In: Proc. ICCAD.

# Scalability on Full-chip Layout

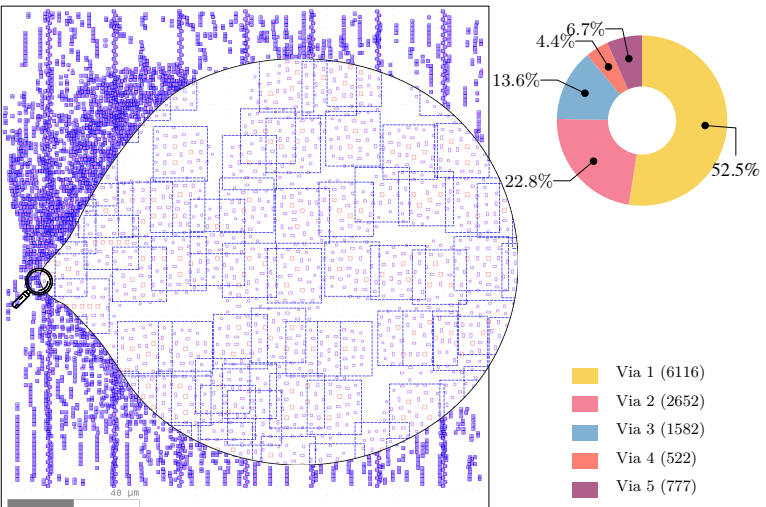


- Tested on  $10\mu\text{m} \times 10\mu\text{m}$  layout.

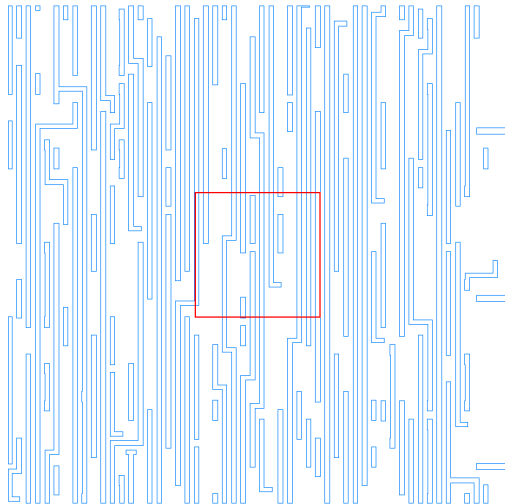


- DMO(1) – Single GPU card;
- DMO(8) – 8 GPU cards

# Results on ISPD 2019 datasets

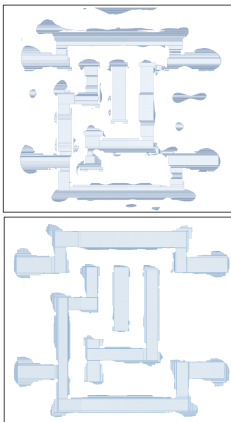
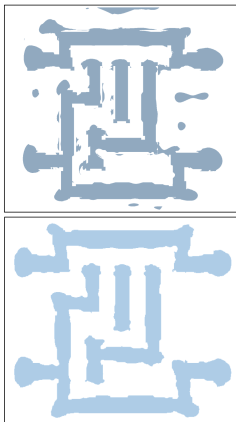


# New Challenges



Main issues in full chip layout

- Scalability
- Stitch error



## Main issues in mask manufacturing

- Non-desired "noisy" patterns
- High mask writing runtime

**THANK YOU!**